Generation of high-power soft x-ray radiation fluxes using the Angara-5-1 facility

V. D. Vikharev, S. V. Zakharov, V. P. Smirnov, A. N. Starostin, A. E. Stepanov, M. V. Fedulov, and V. Ya. Tsarfin

Branch of the I. V. Kurchatov Institute of Atomic Energy

The results are reported of experimental and theoretical investigations of the characteristics of x-ray radiation emitted by liners of different types used in the Angara-5-1 facility. A comparison is made of the spectral characteristics obtained experimentally and by calculation. The influence of the dynamics of the liner acceleration on the radiation characteristics is analyzed.

1. INTRODUCTION

The progress made in the development of high-current generators of very high electrical powers ($P \geqslant 10^{12}$ W) is opening up new opportunities for the investigation of inertial thermonuclear fusion. One of the possible approaches involves compression of a thermonuclear target by irradiation with high-power soft x-ray radiation fluxes.[1] The key factor in this approach is the efficient conversion of the electrical energy available from a high-power generator into x-ray radiation. The driver is an electrodynamically accelerated plasma shell[1,2] whose kinetic energy is converted into thermal energy of compressed plasma.

The efficiency of conversion of the electrical energy of generators into the kinetic energy of a collapsing multiwire liner is considered in Refs. 3–5. Numerical calculations of the efficiency of conversion in the case of Blackjack-5 and PITHON generators are compared in Ref. 3 with the results of experiments on liners made of thin Ti and Al wires. It is shown there that the agreement with the experimental results is good, although it is assumed in these calculations that the liner wires move in a compact manner as one unit. However, it is known from the experimental results[4,6–8] that the acceleration dynamics of wire liners is much more complex and it is not possible to achieve a completely compact motion of the individual wires. Continuous gaseous or condensed cylindrical liners can be accelerated in a more compact manner, but once again problems are encountered in ensuring a homogeneous distribution of the current in the shell, which limits the power of the x-ray radiation generated in this way.

The present paper reports a comparative analysis of the characteristics of soft x-ray radiation of a plasma generated in the multimodule Angara-5-1 facility, where the liner load is in the form of sets of aluminum, copper, or tungsten wires, or supersonic ring-shaped gas jets.

2. DESCRIPTION OF EXPERIMENTS

The radiation generation experiments were carried out using the multimodule Angara-5-1 facility[9,10] with a generator output power of 6 TW. The facility consisted of eight identical modules in the form of a double shaping line with water insulation, connected to a shared load.

In these experiments the rms scatter of the operating times of the eight modules of the Angara-5-1 facility usually was less than 12 ns, which made it possible to pass current pulses with a rise time 90–100 ns through the liner. Electrical pulses from the shaping line were transmitted along vacuum coaxial lines with magnetic self-insulation to an energy concentrator which collected the electrical power delivered to the liner. The distance over which the energy was transported in these vacuum lines was $L \approx 3$ m and the inductance of the vacuum channel was 20 nH. Rigid positioning of the liner during evacuation of the reactor chamber containing the concentrator was ensured by special compensators which eliminated the influence of mechanical displacements of the cathode lines of the exit units of the modules.[10]

A multiwire liner consisted usually of 6–24 thin wires distributed uniformly on the generator of a cylinder with a diameter 15–30 mm and 30 mm high. The diameters of the aluminum, copper, and tungsten wires were 30, 14, and 6 μm, respectively. The running mass of the liner M_l (the number of wires) was selected to ensure the optimal coupling of the generator to the load[11] and was varied within the range 100–300 μg/cm. The construction of the end electrodes and the wire mounting technique ensured that the relative positions of the wires were accurate to within 0.1–0.2 mm. The wire assembly was mounted directly above the cathode current collector in such a way that the liner was above the interelectrode gap separating the disk anode from the cathode. The end electrodes of the liner and the return current conductors were destroyed in each shot.

A hollow supersonic xenon jet was formed by a ring-shaped nozzle. This nozzle was attached to the exit of an electromagnetic valve in the cathode part of the target unit of the vacuum concentrator. The gap between the cathode and anode was 10 mm. Xenon was prevented from entering the interelectrode gap in the concentrator by pulsed formation of a gaseous shell and the anode was a grid consisting of copper wires 0.1 mm in diameter, which was practically transparent to the gas jet.

The nozzles employed formed a supersonic hollow jet with an outer diameter of 30 mm and an inner diameter of 24 mm; the jet traveled at a velocity corresponding to the Mach number $M = 5$. The delay in triggering the accelerator relative to the moment of evaporation of the electromagnetic valve was usually ≈ 1 ms, which ensured that the running mass of the jet was 130–140 μg/cm.

We used a wide range of electrical engineering sensors in a standard system for electrophysical diagnostics described in Ref. 12 (about 50 shunts, Rogowski loops, and magnetic loops); the signals from these sensors provided information on the operation of the individual modules, their synchronization, and parameters of the electrical pulse in various parts of the vacuum transport line and in the target

unit of the vacuum concentrator. The currents supplied to the liner were measured with the aid of shunts and Rogowski loops located in the section between the liner and the cathode collector, and also in some cases at the anode collector at a distance of 12 cm from the liner axis. The voltage across the cathode collector was measured with an inductance sensor located on the support of the concentrator.

The amplitude of the voltage across the liner unit was usually 0.6–0.9 MV when the anode current was up to 3.5 MA. The electrical energy deposited in the load was 200–220 kJ. The amplitudes of the anode and total currents from the eight modules at the entry to the vacuum transmission line were practically the same up to $t = 150$ ns from the beginning of the current pulse, i.e., practically until the collapse of the shells, indicating that the electron leakage currents in the vacuum lines with magnetic self-insulation were low and that the efficiency with which the energy is transported from the generator to the load was high. The electrical pulses obtained from the electrical engineering sensors and from detectors used in the physical diagnostic systems were recorded digitally employing a KIIU-5 data and measuring system. Oscillograms were analyzed using an SM-4 computer. Some of the "fast" signals were recorded using SRG-6 oscilloscopes with a pass band 2 GHz.

The liners were found to be sources of intense visible, vacuum ultraviolet, and soft x-ray radiation both at the moment of collapse and during the acceleration stage. Therefore, the physical diagnostic systems used in the Angara-5-1 facility included fast-response calibrated semiconductor detectors of the soft x-ray radiation, a set of vacuum x-ray diodes fitted with x-ray filters to measure the radiation in the ultraviolet range, a four-frame x-ray camera based on open image converters with microchannel plates, and a four-hole pinhole camera.[13]

Special attention was paid to the determination of the most important characteristic, which was the energy of an x-ray pulse. The precision and reliability of these measurements were improved by employing several methods. A rough estimate of the x-ray radiation energy was obtained and simultaneous visualization of its source was ensured using the pinhole camera with an aluminized Mylar film as the recording medium.[13] The image of a pinch was recorded by the evaporation of the aluminum coating on this film and its energy was estimated by calculating the evaporation energy. This method yielded results which were significantly (severalfold) overestimated. Much more accurate values of the x-ray radiation energy, which agreed to within 20% with one another, were obtained by the following methods: direct determination with microchannel thermocouple calorimeters, a thin-film bolometer with a time resolution of 1 ns, and microchannel vacuum x-ray diodes, followed by subsequent analysis of the results allowing for their spectral characteristics. The last two methods gave results which agreed to within 5–10%.

An x-ray image of the plasma was recorded with the three-channel pinhole camera fitted with various x-ray filters which provided a spatial resolution of at least 30 μm.

The x-ray radiation spectrum in the range $2 \leqslant \lambda \leqslant 19$ Å was recorded with a panoramic spectrograph containing a convex mica crystal (the lattice constant of the mica crystal was $2d \approx 20$ Å and the radius of bending was 25 mm) and the UFSh-S photographic film,[13] and with a diffraction-grating

spectrograph operating in the photon energy range from 100 to 1500 eV. Visible radiation was prevented from reaching the photographic film by placing a beryllium filter 20-μm thick on the entry slit of the crystal spectrograph. A multistage x-ray attenuator (consisting of between one and nine layers of 3-μm-thick Mylar) made it possible to calibrate the UFSh-S photographic film in each experiment. When the vacuum ultraviolet spectrograph was used, its entry slit (whose width was 20 μm) was placed at a distance of 7 m from the liner.

The influence of the dynamics of the accelerated shell on the characteristics of the emitted x-ray radiation was investigated employing an optical diagnostic system comprising SFÉR-2 and M-4 image-converter streak cameras. The SFÉR-2 camera[14] made it possible to carry out optical scans of the line radiation and the multiframe M-4 camera yielded between 3 and 5 consecutive photographs of the image of the liner radiation with a resolution of 3 ns in time and 0.2 mm in space. Moreover, the optical system of the Angara-5-1 facility included a laser probe system which made it possible to record several consecutive (in time) shadow or schlieren photographs of the plasma by exposures lasting 1–2 ns (Refs. 7 and 15).

The experiments carried out using wire liners demonstrated that the passage of a current from the Angara-5-1 generator exploded the wires so that each of them was converted by thermal expansion into a plasma channel typically of ~ 1 mm transverse size. Under the influence of the magnetic field forces the plasma was set in motion and began to accelerate toward the liner axis. In this process the electrical energy from the current generator was converted equally into the kinetic energy of motion of matter and into the energy of the magnetic field. A dense and hot pinch formed on the axis of the system and this pinch emitted strongly in the soft x-ray part of the spectrum.[16]

The wires reached the final velocity of $(4–7) \times 10^7$ cm/s and collapsed at a moment corresponding approximately to the maximum value of the current. A dense and hot plasma pinch (Fig. 1) then appeared at the position of the wire axis and a flash of soft x-ray radiation began. We recorded oscillograms of the current, voltage, and soft x-ray radiation pulses using various filters; the results obtained in one of the experiments are presented in Fig. 2. The duration of the radiation pulses recorded by detection of photons of ≈ 0.3 keV energy was ≈ 60 ns and it decreased to 30–40 ns when photons of 1 keV energy were recorded. Typical final transverse size of the emitting plasma pinch, measured using the x-ray pinhole photographs (Fig. 1), was $R_f = 1.5$–3 mm. When the initial liner diameter R_i was smaller, the resultant pinch had a smaller transverse size. The ratio of sizes was $R_i/R_f \approx 10$ and was practically independent of the initial liner radius. The collapse of the plasma was followed by its thermalization and the kinetic energy was then converted into thermal energy of the compressed plasma. The total radiation energy emitted per pulse was measured with a foil bolometer and, in the case of aluminum liners, it was 50–80 kJ, depending on the experimental conditions.[17]

The leading edges of the oscillograms of the x-ray radiation signals had a characteristic inflection at 15–30 ns before the signal maximum. At the same time a slit scan of the motion of the Al liner indicated that radiation was emitted on the axis of the assembly before significant displacement of
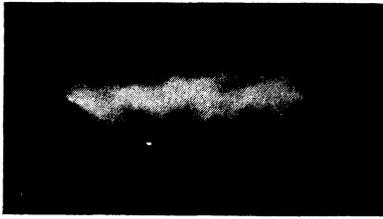
FIG. 1. X-ray pinhole photographs of an aluminum liner.

FIG. 3. Oscillograms of the x-ray radiation pulses obtained for two values of the current through an aluminum liner: 1) 2 MA; 2) 3.5 MA.

the outer boundary of the luminous region. When the amplitude of the current passing through a liner was increased, this inflection of the oscillograms became more pronounced (Fig. 3).

The maximum radiation yield (about 100 kJ) was obtained for a tungsten liner.[17] The power of the emitted radiation was then 2 TW. An optical scan of the radiation of such a tungsten liner is shown in Fig. 4.

Measurements carried out by means of filters using pinhole cameras indicated that the temperature of the plasma pinch was 250–400 eV for the aluminum liner and no more than 100 eV for the tungsten liner.[13]

The spectral distribution of the radiation from the aluminum plasma was investigated in a series of experiments in which we recorded simultaneously the signals from several vacuum x-ray diodes covered by different filters. This was done at right-angles to the liner axis. Figure 5 shows the radiation spectrum at a time corresponding to the radiation maximum.[18]

It should be pointed out that the spectrum remained practically constant in time and only its intensity fell. The power of the radiation emitted in this experiment was less than 1.5 TW and it was found that in the range $hv \geqslant 1$ keV the power was 0.3–0.4 TW. The electrical power from the current generator (≈ 5 TW) delivered to the load was higher than the maximum radiation power, indicating that the compression of the aluminum liner was not compact and there was no "sharpening" of the power profile.
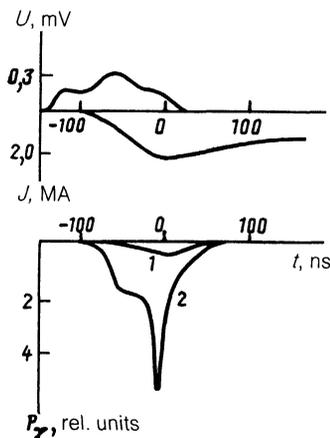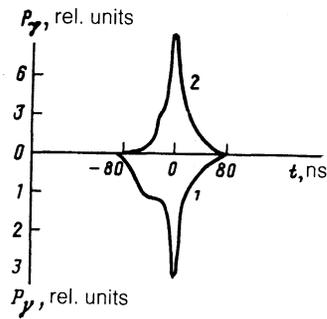

FIG. 2. Oscillograms of the current through an aluminum liner, of the voltage across the liner unit, and of the signals from x-ray radiation detectors: 1) $hv \geqslant 1$ keV; 2) $hv \geqslant 0.1$ keV. The running mass of the liner $M_l = 100 \mu g/cm$; the initial radius $R_l = 1.5$ cm. The moment $t = 0$ corresponds to the maximum x-ray radiation intensity.

The second maximum of the radiation spectrum in the region of $hv \approx 1$ keV was associated with strong line radiation emitted by H- and He-like Al ions. The maximum yield of the radiation at the energies in excess of 1 keV was $W_{>1\ keV} = 10$ kJ. When the rate of rise of the current pulse from the Angara-5-1 generator was increased by a factor of 2–3 (using plasma switches), the proportion of this energy increased by a factor of 2–3.

Figure 6 shows the time-integrated emission spectra of the aluminum and copper plasmas recorded using the spectrograph with a convex mica crystal.[13] Naturally, in the case of the aluminum plasma the line radiation of the H-like Al ions predominated in the investigated spectral range: it was concentrated in the photon energy interval 1.6–2.3 keV. The x-ray emission spectra of the copper liner plasma, recorded in the range 8–13 Å, included 40 distinguishable lines, which were mainly due to transitions in Ne- and F-like copper ions.

3. DISCUSSION OF THE RESULTS OF SPECTROSCOPIC MEASUREMENTS

The availability of fairly detailed information on the spectral characteristics of the radiation emitted by the aluminum liners made it possible to determine the parameters of the plasma pinch in the maximum compression stage where a more or less homogeneous plasma cylinder with a radius $R_f \approx 1$ mm was formed. This stage lasted considerably longer (≈ 50 ns) than the characteristic times for the establishment of the ion composition populations of the excited levels, so that we could use the steady-state approximation. It was assumed that the radial distribution of the plasma was homogeneous.
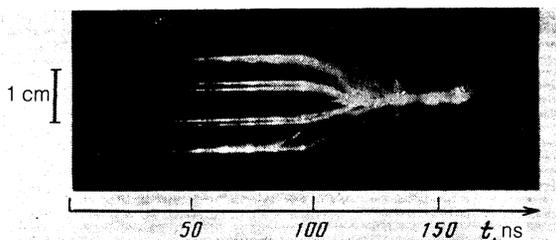

FIG. 4. Slit scan of the motion of a tungsten liner ($M_l = 100 \mu g/cm$, $R_l = 1.5$ cm).

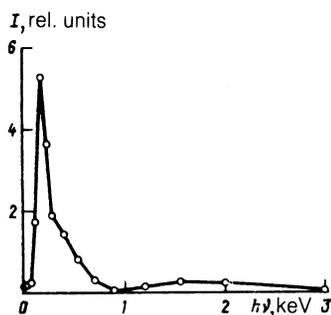FIG. 5. Reconstructed emission spectrum of an aluminum liner plasma $(M_l = 100\,\mu\text{g/cm}, R_i = 1.5\text{ cm})$.

We now consider some approximate calculations of the spectral distribution of the emitted radiation. We can easily show that the characteristic time needed to establish an ionization equilibrium is considerably less than the characteristic time of a change in the temperature of the electron component T_e and of the ion density N_i at any point in the plasma during the collapse period, i.e., the intensity of the radiation and its spectral composition at any time are governed entirely by the distributions of T_e and N_i. It should be

noted that the temperature of the ionic component influences the radiative transfer and then only if the Doppler broadening of the lines is the dominant effect.

A rough estimate of the radiation parameters can be obtained by assuming that at each moment of time the region in space containing the emitting plasma is bounded by a cylindrical surface with a radius R, and the distributions of T_e and N_i within this region are uniform. Let us consider how the radiation depends on T_e, N_i, and R in the case of an aluminum liner. In these calculations we use a model described in Ref. 18. In this model the most serious assumption is the homogeneity of the plasma: it is postulated that the ionic composition of the plasma and the populations of the levels are spatially independent.

Calculations of the relative concentrations of the aluminum ions and of the average charge confirm the natural assumption that, in the investigated range of the densities $(10^{18}-10^{20}\text{ cm}^{-3})$ and temperatures $(200-500\text{ eV})$, the state of the plasma is far from the thermodynamic limit, so that an increase in the density results in a considerable shift of the ionization equilibrium in the direction of stronger ionization and not vice-versa, as would follow from the Saha relationship. A characteristic feature of the spectral composition of the emitted radiation practically throughout the investigat-
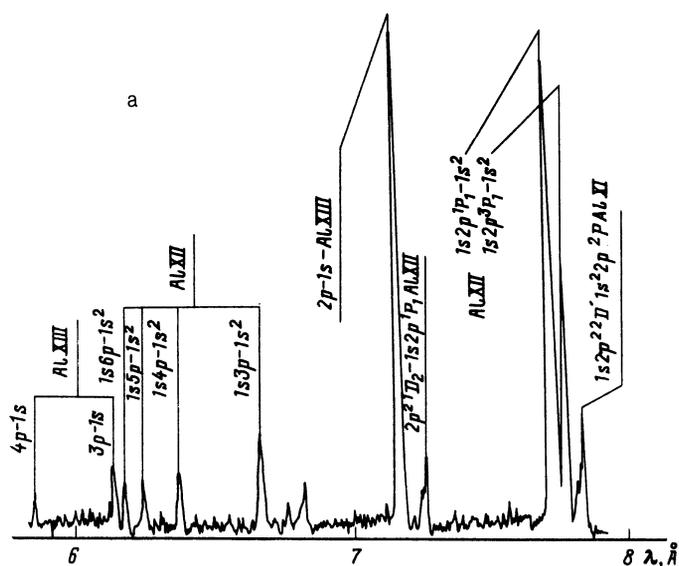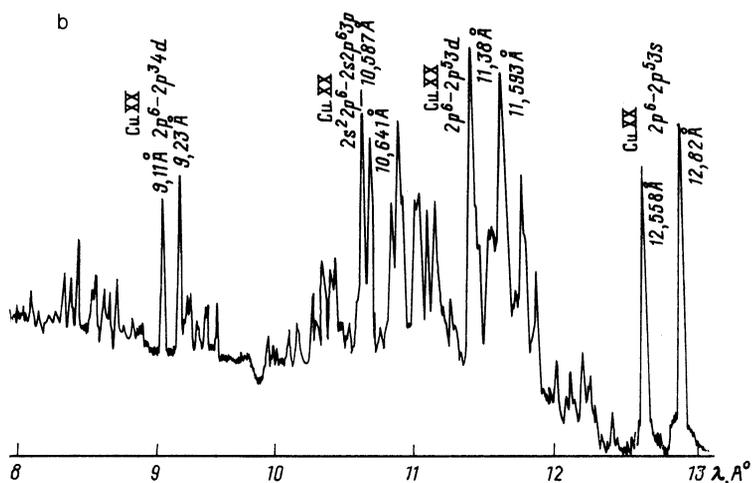

FIG. 6. Emission spectra of a plasma formed from liners: a) Al; b) Cu; $M_l = 100\,\mu\text{g/cm}, R_i = 1.5\text{ cm}$.

634   Sov. Phys. JETP **72** (4), April 1991

Vikharev *et al.*   634

ed range of T_e and N_i is the separation of the spectrum into two parts. At low values of T_e and N_i the lf part of the spectrum is mainly due to the line radiation from Li-like ions. The main contribution comes from the transitions of optical electrons between the states with the principal quantum numbers n amounting to 3 and 2 (transition energy $\Delta E = 0.25$ keV). The hf part at low values of T_e is mainly due to the $n = 2 \rightarrow n = 1$ transitions in He-like ions, i.e., the radiation is concentrated in a narrow energy interval $h\nu = 1.6$ keV. At $T_e = 200$ eV the total intensity of the lf part of the spectrum exceeds the intensity of the hf part throughout the investigated range of N_i, although the concentration of the Li-like ions is within 4%. Naturally, the reason for this is the proximity of the values of ΔE and T_e, whereas the excitation of He-like ions is relatively unlikely.

An increase in the temperature and density reduces strongly the concentration of the Li-like ions so that at high values of T_e and N_i the lf part of the spectrum (where $h\nu < 1$ keV holds) is dominated by the recombination and bremsstrahlung radiations whose intensities are practically proportional to the density (in contrast to Ref. 19, in these calculations the absorption of the photons in the continuous part of the spectrum was allowed for). In the hf part of the spectrum the recombination radiation begins to play an increasing role and then the line radiation by the H-like ions takes over. In view of the low value of T_e compared with the energy of the line radiation emitted by the He-like ions, the intensity of this radiation increases rapidly with temperature, so that determination of the ratio of the intensities in the hf and lf parts of the spectrum provides a good method for estimating the time dependence of the temperature (we denote this ratio of intensities by η and bear in mind that the energy dividing the two parts is 1 keV). However, the method used in such calculations should be more rigorous than that described in Ref. 18.

Figure 7 shows the results of a calculation of the spectral intensity obtained for $T_e = 200$ and 250 eV ($N_i = 4 \times 10^{19}$ cm^{-3}). The radiation intensity is represented by a histogram with the intensity averaged over intervals 200 eV wide. This does not apply to the range $h\nu > 2$ keV, where even in the case of the H-like ions the radiation is practically continuous. At $T_e = 200$ eV the calculated value of η is 0.22, whereas at $T_e = 250$ eV it rises to 0.75. However, we must bear in mind that the experimental results (Fig. 3) indicate that the time interval during which the radiation corresponding to the hf part is emitted is approximately half the whole emission time. Moreover, as demonstrated by an analysis of the ratios of the intensities of the lines emitted by the He- and H-like ions,[17] a plasma emitting radiation is clearly inhomogeneous: near the axis the values of T_e and N_i are considerably higher than at the periphery. In any case, better agreement between the calculations and the experimental results requires further improvement in the experimental method (determination of the spectral characteristics over the shortest possible time intervals) as well as improvements in the calculation model.

Much more information on the spectral characteristics of the aluminum liner plasma radiation can be obtained from calculations using a complete radiation–collisional model in which an allowance is made for radiative transfer in the spectral lines and in the continuum. We developed a detailed
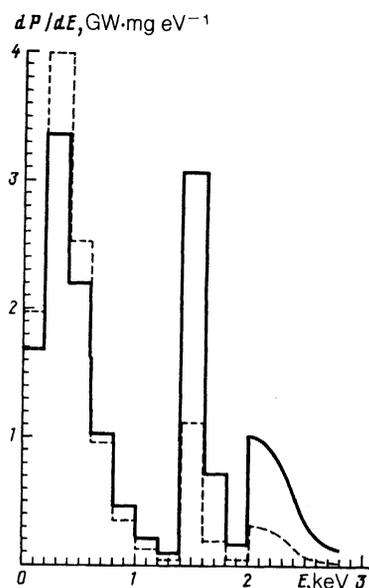

FIG. 7. Histogram of the spectral distribution of the radiation emitted by an Al liner, calculated assuming that $T_e = 200$ eV (dashed line) and $T_e = 250$ eV (continuous line); $N_i = 4 \times 10^{16}$ cm^{-3}.

model of level-by-level kinetics of the H-, He-, and Li-like aluminum ions and a numerical method which can be used to tackle this problem. In the kinetics we allowed for the fine splitting of the levels of the H- and He-like ions with principal quantum number $n \leqslant 3$ and of the Li-like ions with $n \leqslant 5$. The levels of other aluminum ions were ignored because under our conditions their populations should be negligible. The kinetic equations were solved together with the equation for radiative transfer in cylindrical geometry. In this formulation of the problem the steady-state populations in the radiation field are governed by the spatial distributions of the temperature and density, which are assumed to be homogeneous, and by the spatial distribution of the plasma velocity, which is assumed to be a linear function of the radius. An allowance for the motion is very important, because the Doppler shift can alter greatly the optical thickness of the plasma in the resonance lines, the ratio of the intensities of some of the lines used in plasma diagnostics, and the spectral profile of the line radiation. Our model thus has four parameters which determine the spectrum of the emitted radiation: the temperature T_e, the plasma density ρ, the final cylinder radius R_f, and the velocity of motion of the boundary v. In our calculations R_f was assumed to be 1 mm.

This physical model makes it possible to compare the predictions not only with the experimental data on the total radiation power and on the ratios of the energies emitted in the soft and hard parts of the spectrum, but also with the experimental values of the ratios of the intensities of some of the spectral lines and, in the case of the resonance line of an He-like ion, also with the experimentally determined profiles of the emitted radiation lines.

We were able to match the calculated values of the ratios of the intensities of the spectral lines, the total radiation power P, and the ratio η only by allowing for the plasma motion and assuming that $\rho = 2.3 \times 10^{-3}$ g/cm^3, $T_e = 240$ eV, and $v = -2.5 \times 10^7$ cm/s. Table I shows how the calculated and experimental values of the model parameters compare. The calculated emission spectrum is shown in Fig. 8.
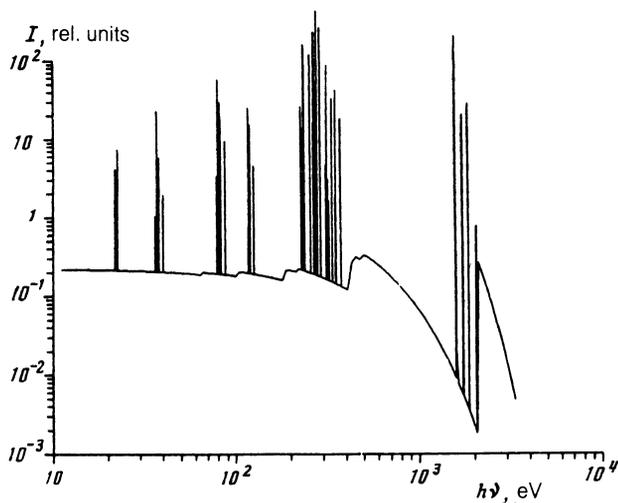
FIG. 8. Emission spectrum of an Al liner calculated using the complete radiation-collisional model allowing for radiative transfer.

We can see from Table I that the calculated and experimental ratios of the spectral line intensities do not match when the plasma velocity is zero.

If we allow for the plasma motion, we find that there is a major change in the spectral line profiles. Figure 9 demonstrates the profile of the resonance and intercombination lines of the He-like Al XII ion obtained experimentally and also by the two calculation versions described above. The line profile calculated allowing for the plasma motion agrees much better with the experimental results. It therefore follows that the experimental data on the spectral characteristics of the radiation taken as a whole agree best with the calculations made allowing for the plasma motion. It is understood that the interpretation of the experimental data in the present paper ignores two important circumstances: they are the plasma inhomogeneity and the time dependences of its parameters. Undoubtedly, a real plasma (as demonstrated by pinhole photographs) is inhomogeneous, but the available experimental data are insufficient to draw reliable conclusions on the nature of this inhomogeneity. Clearly, the most likely is an irregular distribution (over the volume of the pinch) of hotter and denser regions, whose total volume is small compared with the pinch volume. Moreover, as pointed out already, the measurements indicated the time

TABLE I.

	$V=0$	$V=-2,5\cdot10^7$ cm/s	Experiments
P, TW	1,09	1,3	1,2
η	0,49	0,52	0,33
$\dfrac{R(\text{He})}{I(\text{He})}$	0,841	2,35	2,38
$\dfrac{R(\text{H})}{R(\text{He})}$	0,58	0,15	0,16
$\dfrac{3(\text{H})}{R(\text{H})}$	0,093	0,052	0,075

Note. The following notation is used in the above table: $R(\text{He})$ is the intensity of a resonance line of the He-like Al XII ion emitted as a result of the $1s2p\ ^1P_1-1s^2\ ^1S_0$ transition; $I(\text{He})$ is the intensity of an intercombination line of the He-like Al XII ion due to the $1s2p\ ^3P_{0,1,2}-1s^2\ ^1S_0$ transition; $R(\text{H})$ is the intensity of the resonance line of the H-like Al XIII ion due to the $2p-1s$ transition; $3(\text{H})$ is the intensity of the $3p-1s$ line of Al XIII.
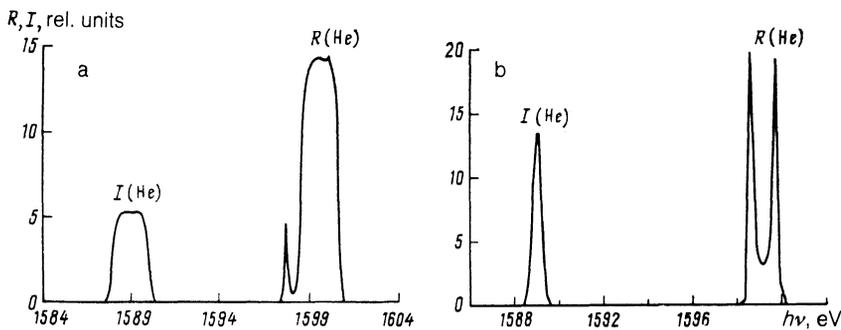
during which the photons are emitted in the hard part of the spectrum is approximately half the total emission time. Therefore, the hypothesis that a plasma filament is inhomogeneous is at present a reasonable compromise. Further progress in the interpretation of such experiments will depend on the development of a calculation model and on improvements in the spatial and temporal resolution of the experimental methods.

4. CHARACTERISTICS OF THE DYNAMICS OF FAST LINERS

A qualitative investigation of the dynamics of collapse of a wire liner was reported in Ref. 16. It was found that the process of compression occurs in two stages. During the first stage the collapse and thermalization of the plasma precursor on the axis of a wire liner gives rise to a cylindrical plasma channel with a diameter 1.5-3 mm, which was clearly visible in the laser shadow photographs, in the frame-by-frame x-ray pinhole photographs, and in streak photos like those shown in Fig. 10. This figure shows a streak photo obtained at the time corresponding to the first maximum of the signal produced by vacuum x-ray diodes (Fig. 2). During the next $\Delta t \approx 10$-30 ns the bulk of the liner reached the axis and the plasma channel formed earlier on the axis began to contract. As a result, when the bulk of the liner collapsed (corresponding to the second maximum of the signal produced by vacuum x-ray diodes) an inhomogeneous plasma cylinder formed on the axis. It should be stressed that it was at this moment that the strongest x-ray radiation was observed in the time-integrated radiation emitted by the liner. It should be pointed out that qualitatively similar results were reported in Ref. 3 for the Blackjack-5 facility.

The acceleration dynamics of copper wire liners were the same as in the case of aluminum liners. Once again a precursor of the plasma channel appeared before the main pinch. The energy of the radiation emitted by the copper liners reached 85 kJ when the running mass and the initial diameter were optimized to achieve the maximum kinetic energy of the liner for a given degree of compression.

Our experimental results made it possible to accelerate effectively the wire liners and achieve the maximum possible energy deposition in these liners. As in Refs. 6 and 7, we observed precursor-type effects and found that in the case of wire liners the shell did not move in a compact manner.

A theoretical calculation analysis reported in Refs. 5 and 8 indicated that the occurrence of a precursor did not reduce the kinetic energy deposited in the liner, although the energy deposition process became extended in time. However, this reduced greatly the power of the output radiation, because the motion of the plasma to the center lasted essentially as long as the current flow in the liner.

As pointed out already, the understanding of the processes influencing the plasma velocity, its profile, and thickness at the moment of collapse would be necessary for estimating the characteristics of x-ray radiation of the pinch (pulse duration and power). A detailed theoretical analysis[8] showed that the quasistationary accelerated magnetic compression of the light-emitting plasma formed from the wires is not possible in two-dimensional geometry. This is because the whole range of two-dimensional equilibrium states of a plasma in a magnetic field is limited by the relationship between the current density j_z, the plasma pressure p, and the vector potential A_z: $j_z = j_z(p)$, $p = p(A_z)$. The relationship

FIG. 9. Profiles of the resonance R(He) and intercombination I(He) lines obtained experimentally (a) and calculated allowing for the plasma motion (b).

$j_z(p)$ is retained when a radiation-emitting plasma column is accelerated as a whole. However, in this case the plasma and magnetic field parameters should be constant at right-angles to the direction of acceleration, i.e., only the motion of a continuous shell can be compact (such a motion is considered in Ref. 20). In reality, the wire plasma expands in the radial direction under the influence of the Ampère forces.

The plasma compression model can be described qualitatively as follows. During the initial stage of the flow of a megampere current through a liner the wires are exploded thermally and they expand. During this stage the plasma travels at the thermal velocity. Overheating of the outer low-density plasma layers produces a density distribution which is close to a vertical step. As the plasma expands beyond the magnetic field separatrix, the Ampère forces accelerate it in the direction of the wire liner axis. The plasma flows from the wires to the axis.

The density of the flowing plasma increases with the emissitivy of the wire material (because its temperature decreases at a given value of the magnetic field). The radiative losses make the plasma temperature relatively low and the plasma motion in jets is supersonic. The electric current is distributed inhomogeneously over the length of such a jet: the current density per unit length is concentrated in narrow layers whose merging in the vicinity of the liner axis occurs at a radius $R_f \approx 0.1 R_i$.

The analytically considered quasisteady model of the plasma flow shows that the compression of wire liners can be regarded as a gradual flow of matter of the wires to the axis of the whole assembly. In the case of a plasma emitting radiation the contribution made to this radiation by the Joule heating is comparable with the kinetic energy of the plasma, which limits the rise of the power of the x-ray radiation emitted by the liner.

Note the dependence of the plasma flux on the emissivity of the target material.[8] This accounts for the qualitative

agreement between the R–t diagram obtained in the zero-dimensional approximation for a tungsten liner and complete disagreement in the case of an aluminum liner. The flow of the plasma of the aluminum wires is a relatively slow process and a quasisteady pattern of motion is established during a pulse. In the case of the plasma formed from tungsten (whose emissivity is an order of magnitude higher than that of the aluminum plasma) practically the whole of the wire mass becomes entrapped in the plasma flux in a time less than the duration of the current pulse, so that the motion of a tungsten liner is more compact.

The observed x-ray radiation yields are 70–85 kJ in the case of aluminum and copper liners. This demonstrates, in particular, that the energy transport from modules of the Angara-5-1 facility to the vacuum concentrator along lines with magnetic insulation is efficient and, moreover, that the efficiency of conversion of the electrical energy delivered by the facility into the kinetic energy of the liner is high (up to 50%). The experimental values of the power of the radiation emitted by a plasma pinch (1–2 TW) do not exceed the power supplied by the accelerator ($P \approx 4$–6 TW) and the duration of the x-ray signal is 40–60 ns. However, in the case of strongly emitting substances such as tungsten, the precursor effect is weaker and a more compact acceleration of the whole system of wires is possible.

Experiments involving compression of hollow xenon shells with a running mass of about 150 mg/cm were carried out using the Angara-5-1 facility in order to reduce the duration of the x-ray pulses and to increase the output radiation power.[21] It was assumed in these experiments that concentration of the current in the skin layer of a continuous shell should prevent the appearance of a plasma precursor on the liner axis and should reduce the duration of the radiation pulses. Xenon was selected because of its high emissivity, in order to ensure the highest radiation energy.
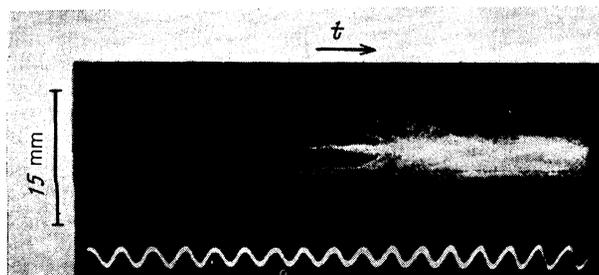

FIG. 10. Streak photo of the radiation emitted by an aluminum liner (the period of the sinusoid at the bottom of the figure is 10 ns).
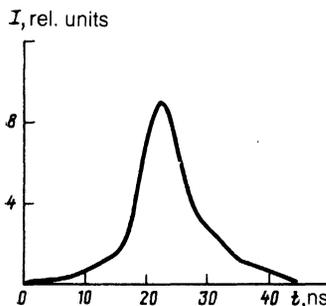

FIG. 11. Oscillogram of a soft x-ray radiation pulse emitted by a xenon liner.
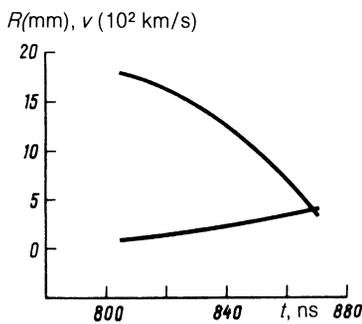
R(mm), v (10² km/s)

FIG. 12. Diagram showing how R and v depend on time t during the motion of a xenon liner shell.

The duration of the x-ray pulses in this case was 20–40 ns at half-amplitude and the actual value depended on the spectral range (Fig. 11). The pulses had a short leading edge whose duration, determined between 0.1 and 0.9 of the maximum intensity, amounted to 5–8 ns. The x-radiation energy, determined by a thermocouple calorimeter closed by a Mylar filter (of thickness $2\,\mu$m) with an evaporated Al film (of thickness $0.1\,\mu$m), was 4.5 kJ. The total radiation energy reached 50 kJ from 1 cm of the liner length. An estimate of the lower limit of the plasma temperature, obtained from these results allowing for the duration of the signals from vacuum x-ray diodes and for the finite size of the pinch (measured using x-ray pinhole photographs on the assumption that the radiation was of blackbody nature), gave 75–80 eV. The power of the radiation emitted by a xenon liner was 2.5 TW and the power density on the pinch surface was 4.5 TW/cm^2.

The diameter of the pinch determined from x-ray pinhole photographs, recorded for photons of the energy $h\nu \geqslant 1$ keV, amounted to 3–4 mm, indicating a tenfold compression of the liner along its radius. The size of the pinch at the cathode was less than at the anode. In the final stage of the formation of the pinch there were instabilities in the form of the $m = 1$ mode (of the firehose type). The shape of this pinch was considerably closer to a cylinder than in the case of multiwire liners.

In the course of collapse the xenon plasma shell accelerated to a velocity of $(4–6) \times 10^7$ cm/s. We determined the R–t diagram of motion of the shell (Fig. 12) by an analysis of the streak photo of the emitted radiation. The minimum size of the region compressed near the cathode was 1.5 mm. In some of the experiments it was found that the final stage of the compression manifested in such photos indicated formation of azimuthal inhomogeneities with the characteristic scale of 2–5 mm.

In the case of continuous strongly emitting multiply charged plasma xenon shells we could distinguish qualitatively two different regimes of the liner formation and acceleration. In the regime discussed in Ref. 20 the plasma heated by the first shock wave cooled rapidly because of the strong emission of radiation. Consequently, the internal thermal pressure of the plasma was considerably less than the magnetic field pressure and the plasma was compressed to the size of a skin layer. Further acceleration of the liner after the passage of the first shock wave occurred in a compact manner.

A different liner acceleration regime was investigated recently.[21] This regime was characterized by a fairly low initial density of the shell matter. The electron–ion energy transfer time $t_{ei} = \tau_{ei}m_i/2m_e$ (τ_{ei} is the electron–ion collision time) behind the front of the shock wave initiated by the magnetic field pressure exceeded the liner compression time. Consequently, the pressure of the ion component of the plasma became comparable with the magnetic field pressure, while the pressure due to electrons was considerably less. The electron temperature was limited by the radiative loss of the energy which the electrons acquired from the ions. The width of the liner during the acceleration stage was greater than the thickness of the skin layer and the internal energy was comparable with the kinetic value. These features of the behavior of the strongly emitting heavy-ion plasma had a considerable influence on the dynamics and stability of the liner compression.

We shall now consider the dynamics of the xenon shell. An increase of the current through such a liner resulted in a short gas breakdown stage in the plasma shell, followed by excitation of a strong shock wave converging on the axis, because of a steep rise of the magnetic field pressure. The shock wave heated primary ions to a temperature $T_i = m_i v^2/3$, and then electrons were heated by electron–ion collisions; the electron temperature in a strongly emitting xenon plasma was limited, as pointed out already, by the radiative losses. A comparison of the rate of energy transfer from the ions to the electrons, and of the radiation power obtained allowing for the experimental values of the plasma velocity behind the shock wave front ($\approx 5 \times 10^7$ cm/s) made it possible to estimate the electron temperature during the first shock wave: $T_e \approx 30$–40 eV. Equalization of the ion and electron temperatures occurred after a time t. In view of the large atomic mass of xenon and the relatively low initial density of the gas ($N_i \approx 10^{19}$ cm^{-3}), the time t in the shell reached 60 ns.

In the inner part of the liner near the axis, where the gas density decreased, the time t was longer. Therefore, throughout the whole collapse process, the shell plasma remained strongly nonisothermal: $T_i \gg T_e$. This nonisothermal behavior became stronger near the liner axis because of an increase in the exchange time and also because of the acceleration of the shock wave which traveled in the presence of a falling density profile. In contrast to the dynamics of compression of a dense strongly emitting liner plasma, in this case the thermal pressure was comparable with the magnetic pressure.

The arrival of the shock wave on the axis was followed by the liner deceleration stage. The temperature of the ions rose almost adiabatically. The energy loss from the plasma was mainly due to the emission of radiation. An increase in the ion temperature increased the electron temperature to 70–90 eV, which was in good agreement with the experimental results. When the liner was compressed by a factor of about 10 along the radius, the state of the plasma approached that of the electron component in laser thermonuclear experiments and the radiation should not have been emitted in the photon energy range $h\nu \leqslant 100$ eV. The time for the emission of the radiation by the dense plasma pinch then decreased to 10–20 ns, which was comparable with the experimentally determined duration of the x-ray radiation pulses and with the pinch lifetime.

In experiments with xenon jets characterized by a high initial gas density it was found that a small prepulse appeared in the oscillogram of the soft x-ray radiation emitted by the liner. Clearly, in this case the liner compression differed from the nonisothermal regime described above, because the time for the energy exchange between the ions and electrons became shorter. The reduction in the electron–ion energy exchange time was responsible for a peak of the radiation immediately after the front of the first shock wave.

5. CONCLUSIONS

In our experimental and theoretical investigations carried out using the Angara-5-1 facility we determined the spectral-time and spatial-energy characteristics of the sources of x-ray radiation formed by compression of liner shells. The relationships governing the "compact" nature of the acceleration of multiwire assemblies and the reasons for departure from such acceleration due to the precursor effect were discussed. The efficiency with which liner kinetic energy was converted into radiation was close to 100%. However, the radiation pulse lengths increased, which limited the power of the radiation.

It was found experimentally and theoretically that in the case of strongly emitting wire liners (made of tungsten) it was possible to improve the compactness of the compression and to increase the radiation power produced in the Angara-5-1 to 2 TW. Collapse of a tungsten liner resulted in 50% conversion of the electrical energies supplied by a current generator into the energy of x-ray radiation (100 kJ per pulse). In the case of aluminum liners a 30% yield of x-ray radiation was obtained in the photon energy range above 1 keV. The spectral maxima of the radiation intensity occurred at photon energies 300 and 1500 eV.

The electrodynamic acceleration of the strongly emitting xenon shells with low initial density made it possible to ensure that the collapse of a liner occurred under conditions producing a strongly nonisothermal plasma. This regime was characterized by the emission of x-ray radiation pulses of 20–30 ns duration with a power up to 2.5 TW and a power density on the surface of the source 4 TW/cm². The emission spectrum was of the blackbody type with a plasma source temperature 80–85 eV.

[1] V. N. Mokhov, V. K. Chernyshev, V. B. Yakubov et al., Dokl. Akad. Nauk SSSR 247, 83 (1979) [Sov. Phys. Dokl. 24, 557 (1979)].
[2] S. G. Alikhanov, L. I. Rudakov, V. P. Smirnov, and I. R. Yampol'skiĭ, Pis'ma Zh. Tekh. Fiz. 5, 1395 (1979) [Sov. Tech. Phys. Lett. 5, 587 (1979)].
[3] J. Katzenstein, J. Appl. Phys. 52, 676 (1981).
[4] H. W. Bloomberg, J. Appl. Phys. 51, 202 (1980).
[5] I. K. Konkashbaev, L. B. Nikandrov, and V. P. Smirnov, Papers Presented at Third All-Union Conf. on Engineering Problems of Thermonuclear Reactors [in Russian], Vol. 1, TsNIIatominform, Moscow (1984), p. 252.
[6] J. Pearlman, E. Chu, W. Clark et al., Proc. Fourth Intern. Topical Conf. on High-Power Electron and Ion Beam Research and Technology, Palaiseau, France, 1981, Vol. 1, publ. by Laboratoire Physique des Milieux Ionises, Palaiseau (1981), p. 271.
[7] L. A. Dorokhin, V. P. Smirnov, M. V. Tulupov, and V. Ya. Tsarfin, Zh. Tekh. Fiz. 54, 511 (1984) [Sov. Phys. Tech. Phys. 29, 304 (1984)].
[8] M. B. Bekhtev, V. D. Vikharev, S. V. Zakharov et al., Zh. Eksp. Teor. Fiz. 95, 1653 (1989) [Sov. Phys. JETP 68, 955 (1989)].
[9] Novosti Termoyad. Issled. No. 3(45), 11 (1987).
[10] E. P. Velikhov, V. P. Smirnov, S. L. Nedoseev et al., At. Energ. No. 6, 234 (1989).
[11] V. V. Bulan, V. V. Zazhivikhin, L. B. Nikandrov, and V. P. Smirnov, Abstracts of Papers Presented at All-Union Seminar on Physics of Fast Plasma Processes, Grodno, 1986 [in Russian], Grodno University (1986), p. 32.
[12] Z. A. Al'bekov, L. E. Aranchuk, A. S. Batyunin et al., Diagn. Plazmy No. 5, 223 (1986).
[13] I. K. Aĭvazov, G. S. Volkov, V. Ya. Tsarfin et al., Vopr. At. Nauk Tekh. Ser. Termoyad. Sintez No. 3, 31 (1987).
[14] V. V. Borisov, A. I. Veretennikov, V. D. Vikharev et al., Prib. Tekh. Eksp. No. 1, 215 (1989).
[15] V. D. Vikharev, L. A. Dorokhin, M. V. Tulupov, and V. Ya. Tsarfin, Prib. Tekh. Eksp. No. 3, 170 (1982).
[16] I. K. Aĭvazov, V. D. Vikharev, G. S. Volkov et al., Fiz. Plazmy 14, 197 (1988) [Sov. J. Plasma Phys. 14, 110 (1988)].
[17] I. K. Aĭvazov, M. B. Bekhter, V. V. Bulan et al., Fiz. Plazmy 16, 645 (1990) [Sov. J. Plasma Phys. 16, 373 (1989)].
[18] M. V. Fedulov, Preprint No. 3433/7 [in Russian], Institute of Atomic Energy, Moscow (1989).
[19] G. S. Volkov, S. A. Komarov, V. P. Sofrygina, and V. Ya. Tsarfin, Pis'ma Zh. Tekh. Fiz. 15(3), 13 (1989) [Sov. Tech. Phys. Lett. 15, 84 (1989)].
[20] S. F. Grigor'ev and S. V. Zakharov, Pis'ma Zh. Tekh. Fiz. 13, 616 (1987) [Sov. Tech. Phys. Lett. 13, 254 (1987)].
[21] V. D. Vikharev, G. S. Volkov, S. V. Zakharov et al., Fiz. Plazmy 16, 379 (1990) [Sov. J. Plasma Phys. 16, 217 (1990)].